JBC RESEARCH ARTICLE

Nutrient-responsive *O*-GlcNAcylation dynamically modulates the secretion of glycan-binding protein galectin 3

Received for publication, January 17, 2022, and in revised form, February 9, 2022 Published, Papers in Press, February 17, 2022,
https://doi.org/10.1016/j.jbc.2022.101743

Mohit P. Mathew[1], **Lara K. Abramowitz**[1], **Julie G. Donaldson**[2], **and John A. Hanover**[1,*]

From the [1]*Laboratory of Cell and Molecular Biology, NIDDK, Bethesda, Maryland, USA;* [2]*Cell Biology and Physiology Center, NHLBI, Bethesda, Maryland, USA*

Edited by Gerald Hart

Endomembrane glycosylation and cytoplasmic *O*-GlcNAcylation each play essential roles in nutrient sensing, and characteristic changes in glycan patterns have been described in disease states such as diabetes and cancer. These changes in glycosylation have important functional roles and can drive disease progression. However, little is known about the molecular mechanisms underlying how these signals are integrated and transduced into biological effects. Galectins are proteins that bind glycans and that are secreted by a poorly characterized nonclassical secretory mechanism. Once outside the cell, galectins bind to the terminal galactose residues of cell surface glycans and modulate numerous extracellular functions, such as clathrin-independent endocytosis (CIE). Originating in the cytoplasm, galectins are predicted substrates for *O*-GlcNAc addition and removal; and as we have shown, galectin 3 is a substrate for *O*-GlcNAc transferase. In this study, we also show that galectin 3 secretion is sensitive to changes in *O*-GlcNAc levels. We determined using immunoprecipitation and Western blotting that there is a significant difference in *O*-GlcNAcylation status between cytoplasmic and secreted galectin 3. We observed dramatic alterations in galectin 3 secretion in response to nutrient conditions, which were dependent on dynamic *O*-GlcNAcylation. Importantly, we showed that these *O*-GlcNAc-driven alterations in galectin 3 secretion also facilitated changes in CIE. These results indicate that dynamic *O*-GlcNAcylation of galectin 3 plays a role in modulating its secretion and can tune its function in transducing nutrient-sensing information coded in cell surface glycosylation into biological effects.

Nutrient sensing is an essential function of glycosylation (1–4). This role is especially important in the context of disease where metabolic imbalances can be detected *via* alterations in patterns of glycosylation (5–10). Glycan synthesis is nontemplate-directed; therefore, glycan structures are dependent on the availability of their carbohydrate components (*i.e.*, sugars). As a result, glycosylation allows cells to "sense" the availability and abundance of sugars and present and display this information in the form of altered glycan patterns. However, it is not well understood how this information is transduced into functional responses. Galectin 3 is a unique protein that provides a link between sensing changes in glycosylation and modulating cellular functions. Galectin 3 recognizes and binds to carbohydrates and hence can detect changes in glycan patterns (11–14). It has also been shown to mediate several cellular functions including clathrin-independent endocytosis (CIE) (15–25). The position of galectin 3 at the interface of glycan pattern detection and modulating cellular function could suggest an important role for galectin 3 as a functional transducer in nutrient sensing.

Galectin 3 is a lectin that is synthesized in the cytoplasm and secreted by "noncanonical" secretion (12, 26–28). Galectin 3 binds to terminal galactose residues and is therefore able to detect changes in cell surface glycosylation patterns (one way in which cells detect and present nutrient information), galectin 3 is unique among the galectin family of proteins due to its ability to multimerize into pentameric complexes (12–14). It has also been shown to drive a number of cellular functions including CIE and cell spreading (15–17, 21–23, 29, 30). These observations uniquely position galectin 3 as a link between detecting nutrient sensing information and functional outcomes. A key element of this function of galectin 3 is that it is an extracellular function and hence requires secretion. Currently, there is little known about how this protein gets across the plasma membrane (26, 31). While export *via* exosomes has been proposed as a means of its secretion (32), a recent genome-wide CRISPR screen for galectin 3 secretory machinery demonstrated that secreted galectin 3 was primarily free and not exosome-bound, suggesting that exosomal export was not the primary secretory pathway (33).

Since galectin 3 is synthesized in the cytoplasm, it could be subject to *O*-GlcNAcylation and interact with *O*-GlcNAcylated proteins. *O*-GlcNAcylation is a ubiquitous posttranslational modification of cytoplasmic proteins. It involves the addition of a single N-acetylglucosamine sugar onto a serine or threonine residue of a protein. There are two enzymes involved in this modification, *O*-GlcNAc transferase (OGT), which adds a GlcNAc residue to a protein and *O*-GlcNAcase (OGA), which removes the *O*-GlcNAc modification (34–37). This modification has been observed on over 1000 proteins and has been shown to dynamically modulate protein signaling and stability in ways that are analogous to phosphorylation (34–37). Importantly, the sugar donor for *O*-GlcNAcylation (UDP-

* For correspondence: John A. Hanover, jah@helix.nih.gov.

GlcNAc) is not only dependent on glucose metabolism but is also influenced by cellular amino acid, fatty acid and nucleotide levels. Thus, *O*-GlcNAcylation plays an important role in nutrient sensing (1, 2, 35, 36).

This study was designed to determine if galectin 3 senses changes in cellular *O*-GlcNAc levels and transduces these nutrient changes to the extracellular environment impacting functional change. Indeed, we find that cellular *O*-GlcNAc levels influence galectin 3 secretion, impacting functional changes in CIE. Our data suggest that galectin 3 can serve as a nexus between nutrient-sensing information represented by cell surface glycosylation and intracellular *O*-GlcNAcylation, integrating information from both these processes, and transducing it into functional biological outcomes.

Results

Galectin 3 secretion is sensitive to changes in cellular O-GlcNacylation

First, we wanted to determine if changes in *O*-GlcNAcylation could impact the ability of galectin 3 to interact with cell surface glycans. A recent review has hypothesized that *O*-GlcNAcylation could contribute to secretion of galectins (38). Thus, we analyzed the secretion of galectin 3 from environments with altered *O*-GlcNAc.

To study the effect of *O*-GlcNAcylation on galectin 3 secretion, we turned to a genetic model of increased *O*-GlcNAc, mouse embryonic fibroblasts derived from OGA knockout mice (39). Knockout of OGA prevents the removal of *O*-GlcNAc residues and leads to an increase in *O*-GlcNAcylation levels. Using an ELISA assay to measure the amount of galectin 3 secreted per cell over the course of a 3-day incubation, we found that in both mouse embryonic fibroblasts (MEFs) derived from males and females, there was a significant decrease in galectin 3 secretion when *Oga* was deleted (Fig. 1*A*). This inhibition in secretion was also observed in immortalized MEFs (Fig. S1).

Next, we looked in a highly proliferative cancer cell line, as glycosylation changes have been proposed to be drivers of cancer progression (14, 40–42). We used siRNA to knock down either OGT or OGA in HeLa cells (Figs. 1*B* and S2*A*). OGT knockdown resulted in a knockdown of both OGT and OGA, without a significant change in global O-GlcNAc levels (Figs. 1*B* and S2*B*), likely due to the *O*-GlcNAcylation-dependent regulation of these proteins themselves (43, 44). Knockdown targeting OGA resulted in decreased OGA levels without significant change in glocal O-GlcNAcylation (Figs. 1*B* and S2*B*). Galectin 3 secretion over a 3-day incubation was measured using an ELISA assay. In both these knockdowns, we observed a significant decrease of galectin 3 secretion consistent with what we had observed in the OGA KO MEFS (Fig. 1*C*).

To further investigate changes in galectin 3 section mediated by *O*-GlcNAcylation, we used chemical inhibitors to disrupt *O*-GlcNAc cycling. Thiamet G inhibits OGA and led to increased levels of *O*-GlcNAcylation, and OSMI-1 inhibits OGT and led to decreased levels of *O*-GlcNAcylation (Fig. 1*D* and S2*B*). Galectin 3 secretion over the course of 2 days wasn't affected by Thiamet G but increased significantly with OSMI-1 treatment (Fig. 1*E*).

These results indicate that loss of OGA inhibits the secretion of galectin 3. Taken together, these data suggests that increased *O*-GlcNAcylation inhibits galectin 3 secretion, whereas decreased *O*-GlcNAcylation stimulates galectin 3 secretion potentially by a sequestration-release model. A possible mechanism is that *O*-GlcNAcylation of galectin 3 signals its sequestration inside the cell, and its deglycosylation is required to release it from the cell. It is possible that thiamet G did not change secretion either because it did not completely inhibit OGA activity and/or because the cells were cultured in a saturated glucose environment, which will be further addressed in Figure 4.

Cellular and secreted pools of galectin 3 are differentially O-GlcNAcylated

Based on the cytoplasmic synthesis of galectin 3 and its primary sequence, we hypothesized that galectin 3 could be directly modified by *O*-GlcNAcylation and/or interact with *O*-GlcNac-modified proteins. To assess if galectin 3 or its interacting partners are *O*-GlcNAc-modified, we performed a wheat germ agglutinin (WGA) pull-down followed by GlcNAc elution of cytoplasmic and whole-cell extracts from HeLa cells. WGA binds terminal GlcNAc residues, and we found that galectin 3 can be pulled down with WGA (Fig. 2*A*).

In order to further investigate if galectin 3 itself can be *O*-GlcNAc-modified, we performed an *in vitro O*-GlcNAcylation assay wherein we incubated recombinant galectin 3 with UDP-GlcNAz and recombinant OGT, we then labeled the azide groups with biotin phosphine that ran the product out on a blot and was detected with streptavidin-IR800. The recombinant galectin 3 was *O*-GlcNAcylated *in vitro* similar to the positive control (Fig. 2*B*). In an effort to further define how *O*-GlcNAc might interact with galectin 3, we enriched for galectin 3 using a specific antibody and did mass spectrometry to identify associated *O*-GlcNAc-modified proteins. This approach identified galectin 3 interacting with several *O*-GlcNAc-modified proteins listed in Table S1. Together, these data suggest that galectin 3 can be modified by OGT and that it interacts with several *O*-GlcNAcylated proteins.

Knowing that galectin 3 can be *O*-GlcNAc modified, we sought to test how this modification could impact secretion. To examine this question, we used a galectin 3 overexpression assay in order to easily detect galectin 3 and monitor secretion in HeLa cells. Three days after transfection, galectin 3-GFP was pulled down from both the cellular and cytoplasmic pools of proteins using the GFPtrap system, which consists of an anti-GFP Nanobody/V_HH coupled to agarose beads, which can be used to efficiently immunoprecipitated (IP) GFP-fusion proteins. Western blot analysis of the IPed proteins (Fig. 2*C*) indicated an RL-2 (*O*-GlcNAc) band overlapping with the galectin 3-GFP band in the cellular pull-down and input lanes. This suggests that galectin 3-GFP is *O*-GlcNAcylated. While the inputs in the secreted pool were too dilute to be detected by Western blot, we were able to detect the pulled down band

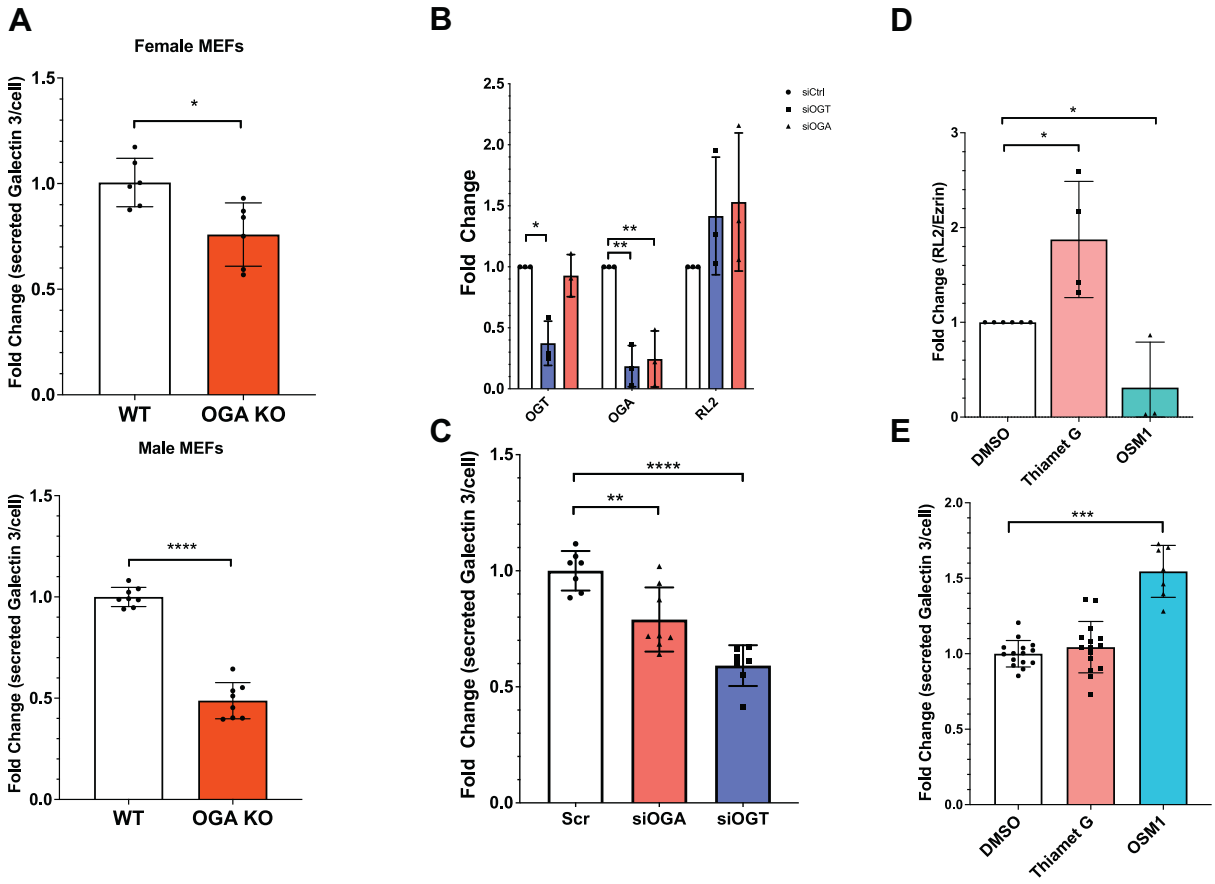

Figure 1. Galectin 3 secretion is affected by *O*-GlcNAcylation. Mouse embryonic fibroblasts from WT and OGA knockout mice were cultured for 48 h and galectin 3 accumulated in the conditioned media was measured by an ELISA assay and normalized to final cell numbers. Knock Out MEFS (*red*) secreted less galectin 3 than wild-type MEFs, this was observed in MEFS obtained from female mice and male mice (*A*). HeLa cells were transfected with siRNA to knockdown either OGA (*red*) or OGT (*blue*). Quantification of Western blotting shows that knocking down OGT or OGA using siRNA transfection leads to decreased OGA levels (OGA knockdown) or a decrease in both OGA and OGT levels (OGT knock down) in both cases there was an increase in *O*-GlcNAcylation observed (RL-2 binding across the whole lane) (*B*). The amount of galectin 3 that accumulated in the conditioned media of control and knock down cells during a 48 h incubation was measured by an ELISA assay and normalized to final cell numbers. Increased *O*-GlcNAcylation by knocking down either OGA or OGT lead to a decrease in galectin 3 secretion measured by the ELISA assay (*C*). Cells were incubated for 72 h with chemical inhibitors for OGT(OSMI-1, *blue*) and OGA(Thiamet-G, *red*). Western blotting shows that inhibiting OGT and OGA using OSMI-1 and thiamet G over a 3-day incubation respectively resulted in a decrease in *O*-GlcNAcylation observed (RL-2 binding across the whole lane) for OSMI-1 treatment and an increase in *O*-GlcNAcylation observed (RL-2 binding across the whole lane) for thiamet G treatment (*D*). The amount of galectin 3 that accumulated in the conditioned media of control and inhibitor treated cells during a 72 h incubation was measured by an ELISA assay and normalized to final cell numbers. This secretion assay indicates that OSMI-1 treatment led to a significant increase in galectin 3 secretion, whereas thiamet G treatment resulted in a small increase in secretion (*E*). At least three independent experiments were carried out with representative blots shown and data expressed as mean ± S.D. (error bars). * indicates $p < 0.05$, ** $p < 0.01$, *** $p < 0.001$, **** $p < 0.0001$ in a one-way ANOVA with a Dunnett's posttest or in an unpaired Student's *t* test. MEF, mouse embryonic fibroblast; OGA, *O*-GlcNAcase; OGT, *O*-GlcNAc transferase.

of secreted galectin 3-GFP. Interestingly, there was very little RL-2 staining corresponding to the secreted galectin-3-GFP pull-down bands. Relative quantification normalizing RL-2 staining to the level of galectin 3 confirmed that there was a significant decrease in *O*-GlcNAcylation level in the secreted pool of galectin 3 (Fig. 2*C*). These results indicate that the *O*-GlcNAcylation of galectin 3 may play a role in its secretion and that the removal of *O*-GlcNAcylation is an important step before galectin 3 can be secreted.

Mutagenesis of potential O-GlcNAc sites alters galectin 3-GFP secretion

Next, we analyzed the protein sequence of galectin 3 for predicted sites of *O*-GlcNAcylation using the YinOYang server (Fig. 3*A*). There were six sites of *O*-GlcNAcylation predicted with a high degree of confidence. Five of these predicted sites clustered in the multimerization region of galectin 3 while the last one (Ser 243) is adjacent to the nuclear export region.

In order to better understand the direct role of *O*-GlcNAcylation on galectin 3, *i.e.*, how changes in *O*-GlcNAcylation of galectin 3 itself affect its secretion, we prepared a set of galectin 3-GFP mutants with various combinations of predicted *O*-GlcNAcylation sites mutated (Fig. 3*B*). These mutants were expressed in HeLa cells, and after a 3-day incubation, the fraction of galectin 3-GFP secreted was measured using a fluorescent plate reader assay (Fig. 3*C*). All the mutants in which all five sites in the multimerization region were deleted or mutated were secreted at a significantly lower level than control galectin 3-GFP. The single mutation near the nuclear transport region did not appear to alter secretion on its own. Further, we found that OSMI treatment did not impact secretion of the deletion null mutant, in which

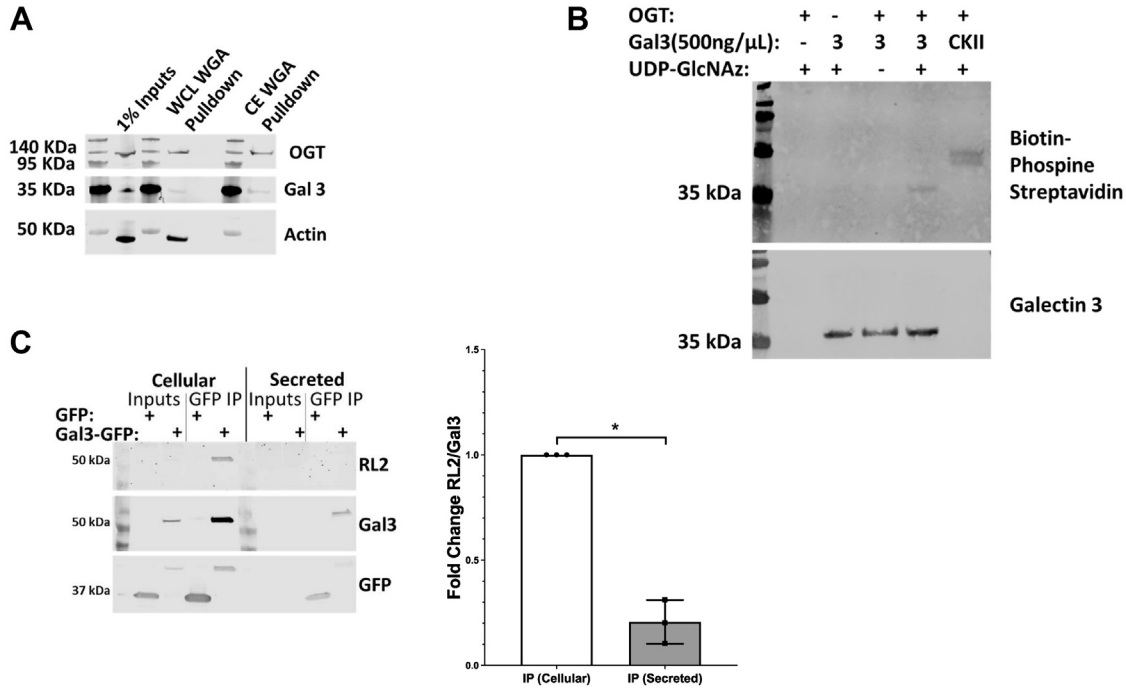

Figure 2. Galectin 3 can be *O*-GlcNAcylated and secreted galectin 3 is preferentially deglycosylated. *O*-GlcNAcylated proteins from whole cell lysates and cytoplasmic extracts were enriched by WGA lectin pull-down and elution using N-Acetylglucosamine. Cell lysates were incubated with agarose beads bound with WGA (a lectin that preferentially binds to N-acetylglucosamine bearing glycoforms), the bound proteins were then eluted by competition using an excess of N-acetylglucosamine to selectively elute terminal GlcNAc residues. Galectin 3 was found to be pulled down in both whole cell lysate and cytoplasmic extract enrichments (*A*). An *in vitro O*-GlcNAcylation assay using recombinant galectin 3, recombinant OGT and UDP-GlcNAz and a Staudinger ligation with biotin phosphine was analyzed by Western blotting with streptavidin. The *in vitro* assay confirms that galectin 3 can be *O*-GlcNAcylated. *B*, galectin 3-GFP was overexpressed in hela cells, after a 48 h incubation galectin 3 from the cells and the conditioned media was then immunoprecipitated using the GFP-TRAP system followed by analysis by Western blotting, HeLa cells expressing just GFP were used as a negative control. Quantifying and normalizing the RL-2 band to the galectin 3 band confirm that secreted galectin 3 is significantly less *O*-GlcNAcylated (*C*). At least three independent experiments were carried out with representative blots shown and data expressed as mean ± S.D. (error bars). * indicates a $p < 0.05$ in an unpaired Student's *t* test. OGT, *O*-GlcNAc transferase.

all five sites in the multimerization region were deleted in addition to a mutation at Ser243, as it did the wild-type Gal3-GFP (Fig. 3*D*). These data suggest that *O*-GlcNAcylation within the multimerization region of galectin 3 plays a role in its secretion. Overall, these results suggest that galectin 3 needs to be first *O*-GlcNAcylated and then deglycosylated in order to be secreted.

Galectin 3 secretion is responsive to nutrient conditions via *dynamic O-GlcNAcylation*

To determine if there was a direct link between nutrient conditions and galectin 3 secretion, HeLa cells were cultured in media with varying glucose concentrations (Fig. 4*A*). When cultured in low-glucose media (1 g/l) and no-glucose media (0 g/l), the HeLa cells secreted significantly more galectin 3 (~3-fold and ~10-fold, respectively) than cells grown in higher glucose concentrations (2–4.5 g/l). Western blot analysis showed that *O*-GlcNAcylation increased with glucose concentration while cellular galectin 3 levels were unchanged (Figs. 4*B* and S3*A*).

The cells were then cultured in media with 0 g/l, 1 g/l, and 4.5 g/l glucose concentrations with or without thiamet G treatment (Fig. 4*C*). When OGA activity was inhibited by thiamet G treatment, there was a significant partial ablation of the nutrient driven increase in galectin 3 secretion in the 0 g/l glucose media condition. This suggests that at least a portion of the nutrient-sensitive change in galectin 3 secretion was driven by dynamic *O*-GlcNAcylation. Western blot analysis confirmed that *O*-GlcNAcylation increased with glucose concentration, and thiamet G treatment leads to an increase in *O*-GlcNAcylation levels, whereas cellular galectin 3 levels were unaffected (Figs. 4*D* and S3*B*).

Because thiamet G does not completely inhibit OGA activity, we also analyzed the MEFs derived from wild-type and OGA KO mice. We found that these cells have a dramatic difference between WT and KO lines (Fig. 4*E*). In the WT MEF cells, there was a significant increase in galectin 3 secretion in cells grown in 0 g/l glucose media (~2-fold increase), whereas there was no statistically significant change in galectin 3 secretion in KO MEFs grown in 0 g/l glucose media as compared with 4.5 g/l. This finding is consistent with a model in which dynamic *O*-GlcNAcylation contributes to nutrient-sensitive changes in galectin 3 secretion.

Changes in O-GlcNAcylation *can alter Galectin-3 functions like CIE*

Our data thus far indicates that *O*-GlcNAcylation impacts galectin 3 secretion. However, it remained unclear if this alteration would impact known extracellular functions of galectin 3 like CIE. In order to determine the physiological

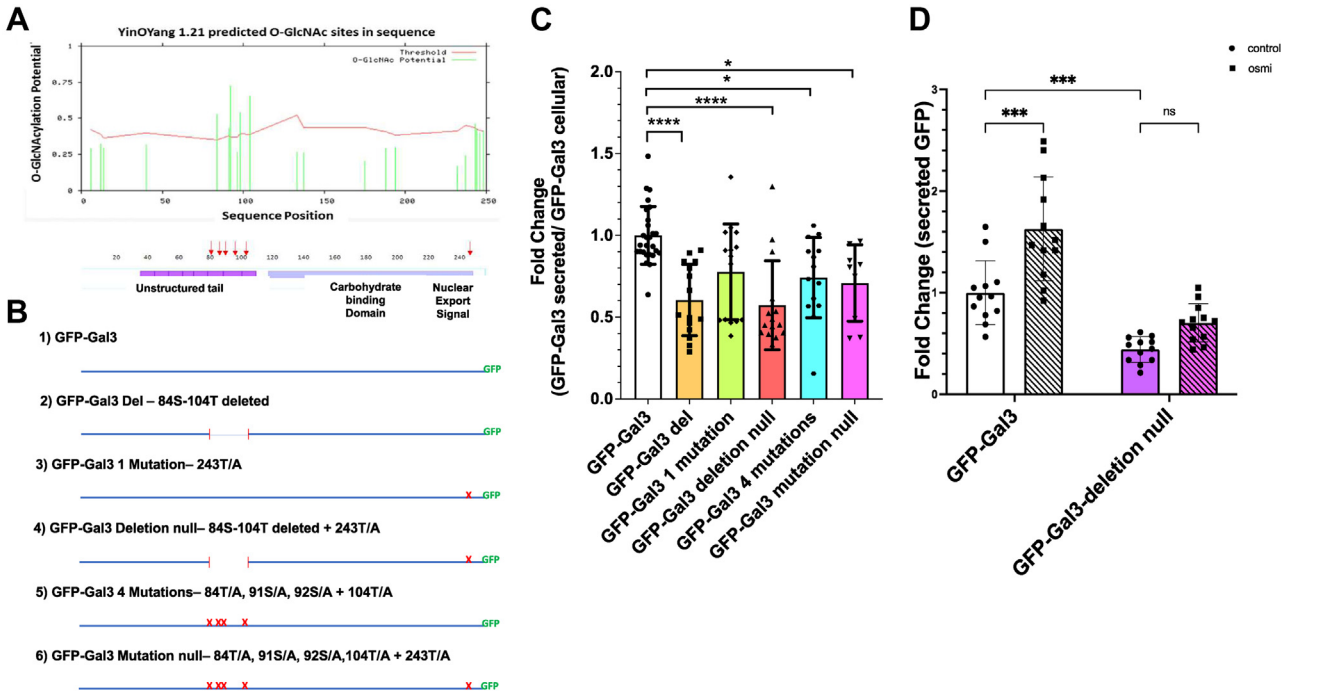

Figure 3. *O*-GlcNAcylation site mutants show direct defects in secretion. Sequence analysis of galectin 3 using the YinOYang software identified five predicted sites of *O*-GlcNAcylation (*A*). *B*, schematic representation of site mutants generated. HeLa cells were transfected with each of these mutant constructs and after a 48 h incubation the galectin 3-GFP accumulated in the conditioned media was measured using a fluorescent plate reader and normalized to fluorescence in the respective cells. This fluorescence-based secretion assay confirms that mutant constructs with either a deletion or mutations of all the sites in the unstructured tail region result in significant secretion defects (*C*). *D*, wild-type galectin 3-GFP (*white bars*) and the deletion null mutant, in which all five sites in the multimerization region were deleted in addition to a mutation at Ser243 (*purple bars*), were treated with 25 μM of OSMI-1 (*diagonal line*) and GFP was measured in the conditioned media after 48 h. At least three independent experiments were carried out and data expressed as mean ± S.D. (error bars). * indicates a $p < 0.05$, ****$p < 0.0001$ in a one-way ANOVA with a Dunnett's posttest (*C*) or a two-way ANOVA with a turkey's multiple comparisons test (*D*).

impact of *O*-GlcNAc on galectin 3 function, we measured the CIE of CD59 after knocking down OGT or OGA (Fig. 5*A*). We observed an increase in CD59 internalization when OGT or OGA was knocked down. The correlation of decreased galectin 3 secretion (Fig. 1*C*) with an increase in CD59 internalization (Fig. 5*A*) supports the model that *O*-GlcNAc changes alter the availability of extracellular galectin 3. Further, we investigated clathrin-mediated endocytosis (CME) of transferrin, which has been shown to be insensitive to changes in galectin–glycan interactions (23) as a control. As expected, CME of transferrin was unaffected by changes in *O*-GlcNAcylation (Fig. 5*B*).

Discussion

How cells sense their nutritional environment and relay that information to modulate physiological outputs remains an essential question. Here we investigated how the galectin, galectin 3, is able to sense nutritional status through *O*-GlcNAcylation and relay that information through interactions with extracellular glycans to ultimately impact CIE (Fig. 6). Our data show that secreted galectin 3 is preferentially deglycosylated (Fig. 2*C*) and that disruption in *O*-GlcNAc cycling leads to altered patterns of galectin 3 secretion. OGA KO MEFs show significant galectin 3 secretion defects, and further, siRNA knockdowns and chemical inhibitors are able to alter galectin 3 secretion in HeLa cells (Fig. 1). These data suggest a link between *O*-GlcNAcylation and nonclassical secretion. Proteins such as FGF and other galectins are also secreted by nonclassical mechanisms and due to their cytoplasmic synthesis could also have their secretion modulated *via* *O*-GlcNAcylation.

Our data further suggests that galectin 3 can be modified by *O*-GlcNAc, and that modification in the unstructured region of galectin 3 modulates secretion (Figs. 2 and 3). Thus, further investigation into the *O*-GlcNAc status of other nonclassically secreted proteins such as FGFs and other galectins is warranted in order to determine if *O*-GlcNAc plays a broader role in modulating the nonclassical secretory pathway. While this study has focused on the potential of direct effects of *O*-GlcNAc on galectin 3 secretion, it remains possible that there are indirect effects as well, through interactions with other *O*-GlcNAcylated proteins and posttranslational modifications.

Importantly, we provide evidence that changes in nutrient status of the cell impact galectin 3 secretion and further that this is through *O*-GlcNAcylation (Fig. 4). These data suggest that glucose entering the hexosamine biosynthetic pathway can ultimately signal to extracellular glycosylation through modulation of galectin 3. Thus, our data indicate that a complex and nuanced role galectin 3 plays as a tunable transducer of nutrient sensing to coordinate physiological adaptations to the nutritional environment. For example, in this study we show that the essential function of CIE is regulated by changes in *O*-GlcNAc. Previous studies have shown

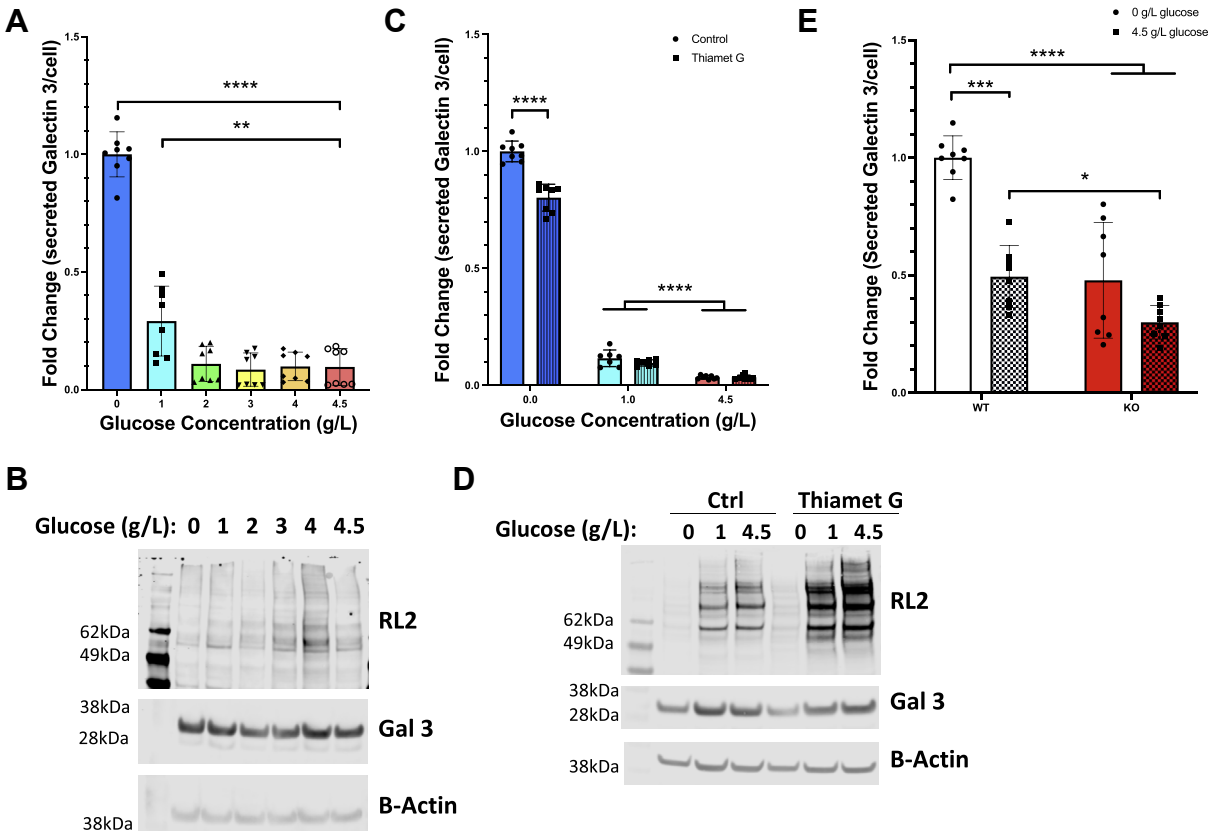

Figure 4. Nutrient conditions have a significant effect on galectin 3 secretion *via* *O*-GlcNAcylation. HeLa cells were grown in different concentrations of glucose for 48 h and the amount of galectin 3 secreted into the conditioned media was measured using and ELISA assay. HeLa cells grown in lower concentrations of glucose (*blue*) were found to secrete significantly more galectin 3 (*A*). Western blots of these HeLa cells grown under different glucose conditions shows a glucose dependent increase in *O*-GlcNAcylation corresponding to glucose concentration (*B*). HeLa cells were then grown in different concentrations of glucose with and without thiamet G treatment (OGA inhibitor, striped bars) for 48 h and the amount of galectin 3 secreted into the conditioned media was measured using and ELISA assay. Thiamet G treatment (*striped bars*) during these incubations leads to a significant partial ablation of the increased galectin 3 secretion observed at 0 g/l glucose (*blue*) (*C*). Western blots of these HeLa cells grown under different glucose conditions with or without Thiamet G treatment shows a glucose dependent increase in *O*-GlcNAcylation corresponding to glucose concentration and increase in *O*-GlcNAcylation corresponding to Thiamet G treatment (*D*). Galectin 3 secretion over 48 h was measured by ELISA assay from conditioned media from mouse embryonic fibroblasts from female WT or female OGA KO mice (*red*) (*E*). The nutrient-sensitive increase in galectin 3 secretion observed in WT MEFs is absent in OGA KO MEFs. At least three independent experiments were carried out with data expressed as mean ± S.D. (error bars). * indicates a $p < 0.05$. **$p < 0.01$, ***$p < 0.001$, ****$p < 0.0001$ in a one-way ANOVA with a Bonferroni posttest. OGA, *O*-GlcNAcase.

that galectin–glycan interactions could be a means by which CIE is modulated (22, 23, 25). We show that disruption of *O*-GlcNAcylation by siRNA knockdown of OGT and OGA leads to a decrease in galectin 3 secretion (Fig. 1*C*) and that the resulting decrease in extracellular galectin 3 leads to an increase in CD59 CIE (Fig. 5). This increased internalization of CD59 was consistent with the trends previously observed when galectin 3 was knocked down in HeLa cells (23). By uncovering the role of *O*-GlcNAcylation and nutrient sensing in regulating galectin 3 secretion and by directly linking *O*-GlcNAcylation disruption to modulation of CIE of CD59, we offer evidence that CIE could be nutrient-sensitive.

Intriguingly, we found that inhibiting OGT with OSMI-1 had the opposite impact on secretion as the deletion of candidate *O*-GlcNAc sites of galectin 3 (Figs. 1 and 3). Further investigation will be necessary to further decipher the mechanism by which *O*-GlcNAc or OGT regulates galectin 3 secretion, but it is possible that there is an uncoupling of catalytic activity with protein availability within a specific nutrient-rich/depleted environment.

In addition to its unique biological niche, galectin 3 dysregulation has also been observed in a wide variety of disease contexts from cancer to diabetes and heart disease (45–52). Hence, understanding the molecular mechanisms driven by galectin–glycan interactions and how galectin 3 secretion is modulated will provide us with valuable insights into how galectins and glycosylation drive the progression of several diseases and how the nutritional environment can impact disease progression.

Experimental procedures

Cell culture, reagents, and antibodies

HeLa and MEF cells were grown in Dulbecco's modified Eagle's medium (Lonza) (4.5 g/l glucose) supplemented with 10% heat-inactivated fetal bovine serum (Atlanta Biologicals), 1.0% 100× glutamine solution (Lonza), and 1.0% 100× penicillin/streptomycin antibiotic solution (Lonza). Cells were maintained at 37 °C in a humidified, 5% CO_2-containing atmosphere.

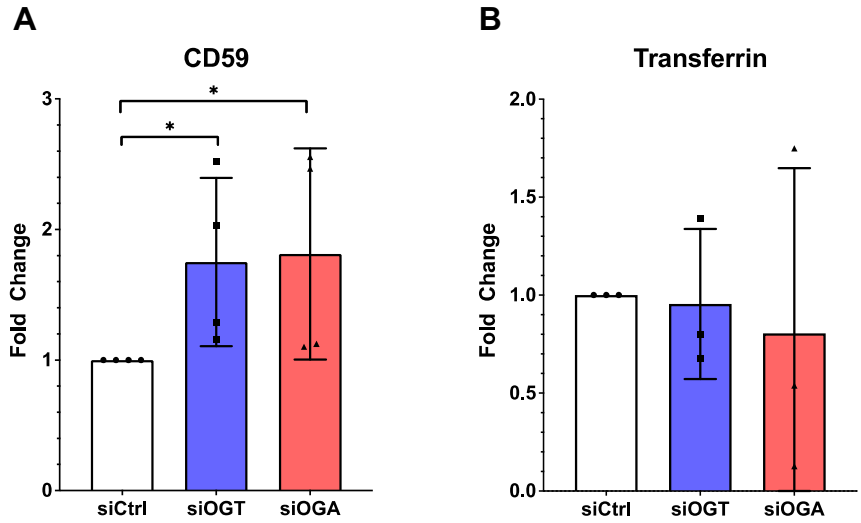

Figure 5. Galectin-3-mediated downstream processes such as CIE are altered by disruptions in *O*-GlcNAc cycling. HeLa cells were transfected with siRNA to knockdown either OGA (*red*) or OGT (*blue*). Clathrin Independent Endocytosis of CD59 was measured using a confocal imaging based antibody internalization assay, was found to increase when *O*-GlcNAc cycling was disrupted by either OGT or OGA knockdown (*A*), whereas clathrin mediated endocytosis of transferrin was not affected (*B*). At least three independent experiments were carried out with representative blots shown and data expressed as mean ± S.D. (error bars). * indicates a $p < 0.05$ in a one-way ANOVA with a Dunnett's posttest.

For glucose treatment, a 100 mM stock solution of glucose (J. T. Baker) in sterile complete culture medium was prepared and used.

For thiamet G treatments, a 2 μg/ml solution of thiamet G (Sigma-Aldrich) in sterile DMSO was prepared, and the cells were incubated in the thiamet G solution for 48 to 72 h before the start of the experiment.

For OSMI-1 treatments, a 2 μg/ml solution of OSMI-1 (Sigma-Aldrich) in sterile DMSO was prepared, and the cells were incubated in 25 μM OSMI-1 solution for 48 to 72 h before the start of the experiment.

Monoclonal antibodies directed toward CD59 (clone p282/H19) were from Biolegend. A monoclonal antibody directed toward galectin 3 (clone A3A12) was from Thermo Fisher. A polyclonal antibody that detects galectin 3 (ab53082) was from Abcam. A polyclonal antibody that detects Ezrin (catalog no. 3145S) was from Cell Signaling. A monoclonal antibody that detects serine or threonine-linked *O*-linked N-acetylglucosamine-RL-2 (ab2739) was from abcam. Anti-OGT (ab177941), anti-OGA (ab124807), and anti-Tubulin (ab6046) were also from abcam. An agarose-conjugated mouse monoclonal anti-galectin 3 (sc-32790 AC) was from Santa Cruz Biotechnology. Alexa 594–conjugated transferrin and all secondary antibodies conjugated to Alexa Fluor 594, 488, 647, 680, and 800 were purchased from Molecular Probes.

Antibody internalization assay

After the indicated incubations, transfections, and pretreatments, cells on coverslips were placed face up on parafilm, and 50 μl of conditioned complete medium containing primary antibody at concentrations of 5 μg/ml for CD59 (Biolegend) or 10 μg/ml Alexa Fluor 488–linked transferrin (Molecular Probes) was added. Coverslips were then incubated either on ice or at 37 °C for 30- to 10-min; incubations were used for transferrin-labeled coverslips. After this, one set of coverslips that was incubated at 37 °C was fixed in 2% formaldehyde (representing total antibody bound both internally and to the surface, T_{tot}), and the other set of coverslips that was held at 37 °C (representing antibody internalized, T_{int}) as well as the set that was kept on ice (null control, T_0) was acid-washed for 40 s using a solution of 0.5% acetic acid, 0.5 M NaCl, pH 3.0, after which these sets of coverslips were fixed in 2% formaldehyde. The cells were blocked for 30 min using a blocking solution of 10% FBS, 0.02% sodium azide in PBS. The coverslips were then labeled at room temperature for 1 h with Alexa Fluor 488–conjugated goat anti-mouse secondary antibody (Molecular Probes), 0.2% saponin, and 2 μg/ml HCS cell mask deep red stain (Molecular Probes) in blocking solution. The coverslips were then rinsed three times in blocking solution and a final time with PBS, and they were then mounted on glass slides.

Coverslips were imaged at room temperature using a confocal microscope (LSM 780 FCS, Carl Zeiss) with a 40× PlanApo oil immersion objective and 488- and 633-nm laser excitation. For each coverslip, six positions were imaged with 2 × 2 tiling with the pinhole kept completely open. For each condition across the six tiled images, at least 100 cells were imaged. All images for each antibody were taken with identical acquisition parameters, which are set based on the control's T_{tot} coverslip and tuned such that the signal was within the dynamic range.

The MetaMorph application (Molecular Devices) was used to quantify the percentage of antibody internalized. Confocal images were separated into the two different channel colors. An antibody channel threshold was set for each condition using its T_0 coverslip images. The T_{int} and T_{tot} conditions were then thresholded, and the integrated signal intensity was measured for the antibody channel. The cell mask channel was autothresholded, and the threshold area was measured. The

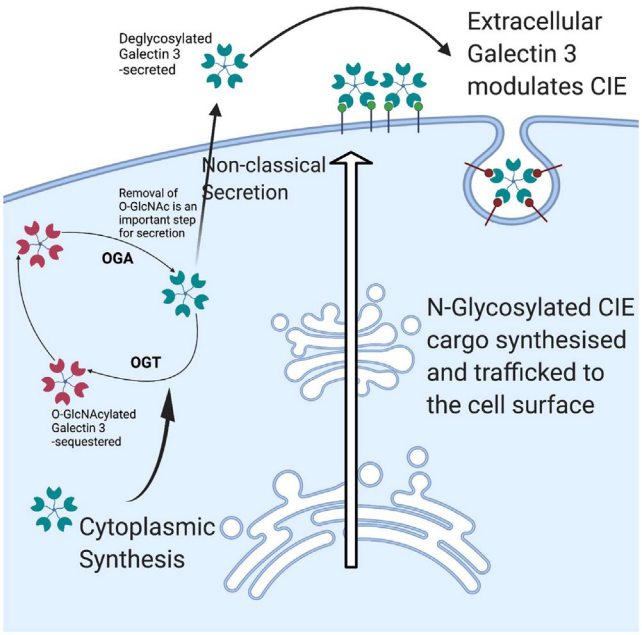

Figure 6. Schematic depiction of the role of galectin 3 in nutrient sensing. Galectin 3 is synthesized in the cytoplasm and then secreted by noncanonical mechanisms. Once outside the cell it binds to terminal galactose residues and can modulate a number of important cellular functions like clathrin independent endocytosis, cell spreading, etc. N-glycosylation is a nontemplate-directed process and as such the glycan patterns that are produced are dependent on the availability of the enzymes and the substrates, as a result changes in nutrient environment are presented as altered glycan patterns. These glycan patterns are detected and bound to by galectins, which can then transduce these changes in pattern into changes in cellular behavior *via* the processes these galectins modulate. The cytoplasmic origin of galectin 3 allows interaction with the *O*-GlcNAcylation machinery. *O*-GlcNAcylation also plays a role in nutrient sensing and is known to dynamically modulate the behavior of numerous proteins. We present a model in which galectin 3 necessitates *O*-GlcNAcylation and deglycosylation for proper secretion. Thus, galectin 3 can integrate nutrient sensing information from both *O*-GlcNAcylation and N-Glycosylation and transduce this information into biological effects. This figure was created using BioRender.

integrated signal intensity for the antibody was then normalized to the threshold area for each image. The percentage internalized is then calculated with the equation, % internal = $100 \times T_{\mathrm{tot/area}}/T_{\mathrm{int/area}}$. Finally, the internal percentages were normalized to the untreated control.

Galectin 3 ELISA secretion assay

Cells were seeded on a 6-well plate at a density of 3×10^5 cells/well in 1 ml of complete medium in quadruplicate with relevant siRNA transfections and chemical inhibitor treatments. After a 48 h or 72 h incubation, the supernatants (*i.e.*, conditioned medium) were collected and spun down at 3000*g* for 10 min to remove any cell debris. Supernatants were then analyzed for galectin 3 content using a human galectin 3 ELISA kit (Abcam, ab 188394) as recommended by the manufacturer. Cells in the well were trypsinized to detach and counted. Galectin 3 in the supernatant was normalized to cell number.

siRNA transfection

Cells were seeded in antibiotic-free complete medium and transfected with a 50 nM final concentration of OGT (Dharmacon, ON-TARGET plus human OGT (8473) siRNA-smartpool), OGA (Dharmacon, ON-TARGET plus human MGEA5 (10,724) siRNA-smartpool), or nontargeting siRNA (Dharmacon, ON-TARGETplus nontargeting pool) using Lipofectamine RNAiMAX (Invitrogen) as recommended by the manufacturer. Cells were used in experiments 48 to 72 h after transfection.

Western blot analysis

Proteins obtained from cells were analyzed by Western blotting. Briefly, after the appropriate treatment (transfection, siRNA treatment, etc.), cells were washed three times in cold PBS, harvested by using a tissue culture cell scraper, and pelleted by centrifugation at 4 °C (1200*g* for 10 min). Pellets were solubilized in RIPA buffer (Abcam), protein levels were measured and normalized using a BCA assay (Thermo Fisher). Proteins were separated by 10 to 20% SDS-PAGE, transferred to nitrocellulose paper, and probed with the following commercial antibodies: anti RL-2 (Abcam), anti-tubulin (Abcam), anti-OGT (Abcam), anti-OGA(Abcam), anti-Ezrin (Cell Signaling), and anti-galectin 3 (Thermo Fisher). Membranes were imaged using LI-COR Odyssey IR imager. Protein bands were quantified using the Image Studio Lite software.

WGA pull-down

Whole-cell lysates were obtained using RIPA buffer for lysis, and cytoplasmic fractions were obtained using the NE-PER nuclear and cytoplasmic extraction reagents (Thermofisher). Hundred microliters/sample of agarose-bound WGA (Vectorlabs) was washed three times in PBS containing 0.2%NP40. One microgram of sample was added to beads and incubated overnight at 4 °C. The next day, the beads were washed four times in PBS containing 0.2% NP-40 for 20 min each. Samples were eluted from the beads using 1 M GlcNAc in PBS containing 0.2% NP-40 incubating for 1 h on ice. After loading dye was added and samples were boiled, samples were processed as described above for Western blot analysis.

Plasmids, primers, and transient transfection

GFP-tagged galectin 3 (pEGFP-hGal3 (Addgene, plasmid no. 73080) was mutated using the Q5 site directed mutagenesis kit (New England Biolabs, catalog number E0554S) and designed primers according to the manufacturer's instructions. Required mutations, deletions, insertions, and combinations of these were generated using the following primers: *GFP-Gal 3 Del (84S-104T deletion)* Forward primer: 5′-GGCCCCTATGG CGCCCCT-3′, Reverse primer: 5′-GGGTGGCCCTGGGTA-GACTC-3′. *GFP-Gal 3 1 mutation (243 T/A)* Forward primer: 5′- CATAGACCTCgccAGTGCTTCAT -3′, Reverse primer: 5′- TCACCAGAAATTCCCAGTTTG -3′. *GFP-Gal 3 Deletion null(84S-104T deletion and 243 T/A):* using the confirmed GFP-Gal 3 Del mutant the primers for GFP-Gal 3 1 mutation (243 T/A) were used. *Insertion (84S-104T, 84S/A,91S/A,92S/A,104T/A)* Forward primer: 5′- gccagccgcccccggagcctaccctgc-cactGGCCC CTATGGCGCCCCT -3′, Reverse primer: 5′-tgtccggcggctgggtaggccccagggccggcGGGTGG

CCCTGGGTAGACTC-3′. *GFP-Gal 3 4 Mutation (84S/A,91S/A,92S/A,104T/A)* using the confirmed GFP-Gal 3 Del mutant the primers for Insertion were used. *GFP-Gal 3 Mutation null (84S/A,91S/A,92S/A,104T/A and 243T/A)* using the confirmed GFP-Gal 3 Deletion null mutant the primers for Insertion were used. *Control silent (124G/G and 125G/G)* Forward primer: 5-GCCTTTGCCTggagggGTGGTGCCTC -3′, Reverse primer: 5′- AGGTTATAAGGCA CAATCAGTGGCCC -3′. *Control random substitution (124G/A)* Forward primer: 5′- GCCTTT GCCTgcgGGAGTGGTGC -3′, Reverse primer: 5′- AGGT-TATAAGGCACAATCAGTGGC -3′.

Sequencing Primers Forward primer: 5′- CGGACTCA-GATCTATGGCAGAC -3′, Reverse primer: 5′- AAACCTC-TACAAATGTGGTATGGC -3′.

Cells were seeded in complete medium. After a 24-h incubation, cells were transfected with GFP-tagged galectin 3 (pEGFP-hGal3) or mutants of it, or pEGFP-N3 (Clontech, catalogue no. 6080-1) at 2.5 μg of DNA/60-mm well using Xtremegene9 (Roche Diagnostics) as recommended by the manufacturer. Experiments were performed 48 to 72 h after transfection.

In-vitro *OGT assay*

The reaction mixture was prepared by mixing 2 μg of recombinant OGT, 3 μg of recombinant galectin 3(Abcam, ab89487), 1 μl of 2 M UDP-GlcNAz and making the volume up to 50 μl with OGT assay buffer (50 mM Tris–HCl, pH 7.5, 1 mM dithiothreitol, 12.5 mM $MgCl_2$). Negative controls were prepared by removing either OGT, galectin 3 or UDP-GlcNAz from the reaction mixture. A positive control was prepared by substituting casein kinase II (NEB, P6010S) for galectin 3 in the reaction mixture.

The OGT assay mixtures were incubated for ∼90 min in a 37 °C water bath. The reaction mixtures were then added to 10K filters and spun at 14,000 rpm for 30 min. The filters were washed with 100 μl of PBS and spun down at 14,000*g* for 10 min twice. To recover the protein, the membranes were flipped and spun down at 1000*g* for 3 min. One microliter of biotin phosphine was added and incubated for 1 h at 40 °C. The samples were then boiled for 10 min in 1× sample-loading buffer, and proteins were separated by 10 to 20% SDS-PAGE, transferred to nitrocellulose paper, blocked in odyssey blocking buffer for 1 h, and probed with streptavidin IR800 and anti-galectin 3 (Abcam). Membranes were imaged using a LI-COR Odyssey IR imager.

In silico *O-GlcNAcylation site prediction*

The galectin 3 sequence was used on the YinOYang 1.2 server to predict site of *O*-GlcNAclation (http://www.cbs.dtu.dk/services/YinOYang/) (53, 54). The server generates a list of predicted sites with varying degrees of confidence.

Galectin 3 immunoprecipitation assay

After a 48-h incubation with or without GlcNAc treatment, cells were rinsed with ice-cold PBS and lysed in 1 ml of ice-cold RIPA buffer (150 mM NaCl, 1% Nonidet P-40, 0.5% sodium deoxycholate, 0.1% SDS, 50 mM Tris, pH 8.0) with protease inhibitor mixture (Sigma-Aldrich). Lysates were centrifuged at 13,300 rpm for 10 min. Supernatants were transferred to fresh Eppendorf tubes. The samples were immunoprecipitated using 15 μg/ml agarose conjugated anti-galectin 3 (Santa Cruz Biotechnology) or agarose protein G beads (GE Healthcare) only. The beads were preblocked for 1 h on ice with 3% BSA (Sigma-Aldrich) in RIPA buffer. After immunoprecipitation, beads were rinsed three times with RIPA buffer and boiled for 10 min in 1× sample-loading buffer.

Mass spectrometric analysis

After Galectin 3 immunoprecipitation, the samples were resolved on SDS-NuPAGE gel and stained with Simply Safe Blue (Invitrogen). Multiple protein bands were excised, destained with 50% methanol in 50 mM bicarbonate, reduced with 20 mM DTT at 57 °C for 45 min and alkylated with 50 mM iodoacetamide in the dark at room temperature for 30 min, and then were digested with 5 ng/ul of trypsin (Promega) at room temperature overnight according to the manufacturer's protocol. The resulting peptides were dried and reconstituted in 0.1% formic acid and desalted by C18 ziptip (EMD Millipore) according to the manufacturer's protocol. The eluted peptides were dried again and dissolved with sample loading buffer (0.1% formic acid, and 5% AcN) for LC-MS/MS analysis.

LC-MS/MS analysis

The digested peptides were analyzed by reverse-phase LC-MS/MS on an Orbitrap Fusion Lumos mass spectrometer (Thermo Scientific) coupled to a Dionex UltiMate 3000 -nLC (Thermo Scientific) liquid chromatography system. Digested proteins were first loaded onto a trap column (Acclaim PepMap 100 precolumn, 75 μm × 2 cm, C18, 3 μm, 100 Å, Thermo Scientific) and then separated on an analytical column (EASY-Spray column, 50 cm × 75 μm ID, PepMap RSLC C18, 2 μm, 100 Å, Thermo Scientific) maintained at a constant temperature (45 °C) and equilibrated with 2% buffer A (0.1 % Formic acid). Peptides were separated with a 55-min linear gradient of 5 to 30% buffer B (100% acetonitrile, 0.1% formic acid) at a flow rate of 300 nl/min. The mass spectrometer was operated in data-dependent mode to automatically switch between MS and MS/MS acquisition. Each full MS1 scan was acquired from 375 to 1500 (120,000 resolution, 4e5 AGC, 50 ms injection time) followed by EThcD MS/MS acquisition (15,000 resolution, 5e4 AGC, 90 ms injection time), and HCD supplemental activation was set to 25% NCE.

All raw data files were searched against UniProt homo sapiens database (downloaded 01/2018) using PD 1.4 software using Sequest H. Trypsin was selected as the enzyme, and two maximum missed cleavages were allowed. Searches were performed with a precursor mass tolerance of 20 ppm and a fragment mass tolerance of 0.05 Da. Static modifications consisted of carbamidomethylation of cysteine residues (+57.021 Da). Dynamic modifications consisted of oxidation of methionine residues (+15.995 Da), deamidation of asparagine deamidation of asparagine and glutamine (+0.984 Da), and GlcNAc attachment to serine and threonine (+203.079 Da).

Four maximal dynamic modifications were allowed. Peptide spectral matches (PSMs) were validated by percolator with the false discovery rate of 1%. The mass spectrometry proteomics data have been deposited to the ProteomeXchange Consortium *via* the PRIDE partner repository with dataset identifier PXD028139.

GFP-trap immunoprecipitation of GFP-tagged galectin 3 mutants

After a 48-h transfection with GFP-tagged galectin 3, mutants cells were rinsed with ice-cold PBS and lysed in 1 ml of ice-cold RIPA buffer (150 mM NaCl, 1% Nonidet P-40, 0.5% sodium deoxycholate, 0.1% SDS, 50 mM Tris, pH 8.0) with protease inhibitor mixture (Sigma-Aldrich). The conditioned media was also collected in some experiments and spun down at 3000*g* for 10 min to remove any cell debris; supernatants were transferred to fresh eppendorf tubes. Cell lysates were centrifuged at 13,300 rpm for 10 min. Supernatants were transferred to fresh eppendorf tubes. The samples were immunoprecipitated using 25 µl bead slurry of GFP-Trap Agarose (Chromotek) (GFP-Trap consists of an anti-GFP Nanobody/V_HH coupled to agarose beads to immunoprecipitate GFP-fusion proteins). The beads were preblocked for 1 h on ice with 3% BSA (Sigma-Aldrich) in RIPA buffer. After immunoprecipitation, beads were rinsed three times with wash buffer (10 mM Tris/Cl pH 7.5, 150 mM NaCl, 0.05 % Nonidet P40 Substitute, 0.5 mM EDTA) and boiled for 10 min in 1× sample-loading buffer, and proteins (2% of input supernatant and 100% of the immunoprecipitate) were separated by 10 to 20% SDS-PAGE, transferred to nitrocellulose paper, and probed with the following antibodies: anti-Ezrin (Cell Signaling), anti-galectin 3 (Abcam), and anti-RL-2 (Abcam). Membranes were imaged using a LI-COR Odyssey IR imager.

GFP-tagged galectin 3 secretion assay

Cells were seeded on a 12-well plate at a density of 5×10^4 cells/well in 1 ml of complete medium in quadruplicate. Cells were transfected with GFP-tagged galectin 3 (Addgene) or a mutant variant of it. After 24 h, the medium was replaced with 500 µl of FluoroBrite Dulbecco's modified Eagle's medium (Life Technologies) supplemented with 10% heat-inactivated fetal bovine serum (Atlanta Biologicals), 1.0% 100× glutamine solution (Lonza), and 1.0% 100× penicillin/streptomycin antibiotic solution (Lonza). Seventy-two hours posttransfection, the supernatants were collected and spun down at 3000*g* for 10 min to remove any cell debris, and 200 µl of the supernatant was transferred to a black 96-well plate in duplicate. The cells were also detached by incubating with 0.25% trypsin for 1 min at 37 °C. Cells were collected, spun down, and resuspended in 500 µl of PBS. Two-hundred microliters of the cell suspensions was also transferred to a black 96-well plate in duplicate. Bulk fluorescence in each well was measured using a Synergy H1 multimode microplate reader (BioTek). After background-subtracting any fluorescence from the medium, PBS, and cell autofluorescence, the fluorescence from the supernatant wells was normalized to the fluorescence in the cell suspension wells.

Statistical analysis

At least three independent biological replicates (independent experiments) were carried out for each experiment, and data were expressed as mean ± SD. In experiments with multiple comparisons, statistical significance was determined using a one-way ANOVA with a Dunnett's posttest to compare means of different samples with the control or a Bonferroni posttest to compare specific pairs of columns. A two-way ANOVA with Turkey's multiple comparison test was used when there were two categorical variables. In experiments with only two conditions, an unpaired Student's *t* test was used to determine statistical significance. The null hypothesis was rejected in cases where *p* values were <0.05.

Data availability

The mass spectrometry proteomics data have been deposited to the proteomexchange consortium *via* the pride partner repository with dataset identifier pxd028139. All other data are contained within the manuscript.

Supporting information—This article contains supporting information.

Acknowledgments—The mass spectrometry experiments were carried out by Yanling Yang and Marjan Gucek at the Proteomics Core Facility, NHLBI, NIH, Bethesda, Maryland, USA. Recombinant OGT was expressed and purified by Agata Steenackers. This work was supported by NHLBI, National Institutes of Health, intramural research program grant Hl006130 and by NIDDK, National Institutes of Health, intramural research program grant ZIADK060103. The content is solely the responsibility of the authors and does not necessarily represent the official views of the National Institutes of Health.

Author contributions—M. P. M. conceptualization; M. P. M. and L. K. A. formal analysis; J. A. H. funding acquisition; M. P. M. and L. K. A. investigation; M. P. M. methodology; J. A. H. supervision; L. K. A. visualization; M. P. M. and L. K. A. writing—original draft; J. G. D. and J. A. H. writing—reviewing and editing.

Conflict of interest—The authors declare that they have no conflicts of interest with the contents of this article.

Abbreviations—The abbreviations used are: CIE, clathrin-independent endocytosis; CME, clathrin-mediated endocytosis; MEF, mouse embryonic fibroblast; OGA, *O*-GlcNAcase; OGT, *O*-GlcNAc transferase; WGA, wheat germ agglutinin.

References

1. Wells, L., Vosseller, K., and Hart, G. (2003) A role for N-acetylglucosamine as a nutrient sensor and mediator of insulin resistance. *Cell. Mol. Life Sci.* **60**, 222–228
2. Wellen, K. E., and Thompson, C. B. (2010) Cellular metabolic stress: Considering how cells respond to nutrient excess. *Mol. Cell* **40**, 323–332

3. Zachara, N. E., and Hart, G. W. (2004) O-GlcNAc a sensor of cellular state: The role of nucleocytoplasmic glycosylation in modulating cellular function in response to nutrition and stress. *Biochim. Biophys. Acta* **1673**, 13–28
4. Chiaradonna, F., Ricciardiello, F., and Palorini, R. (2018) The nutrient-sensing hexosamine biosynthetic pathway as the hub of cancer metabolic rewiring. *Cells* **7**, 53
5. Turner, G. (1992) N-glycosylation of serum proteins in disease and its investigation using lectins. *Clin. Chim. Acta* **208**, 149–171
6. Beisswenger, P. J., Makita, Z., Curphey, T. J., Moore, L. L., Jean, S., Brinck-Johnsen, T., Bucala, R., and Vlassara, H. (1995) Formation of immunochemical advanced glycosylation end products precedes and correlates with early manifestations of renal and retinal disease in diabetes. *Diabetes* **44**, 824–829
7. Wang, J.-Z., Grundke-Iqbal, I., and Iqbal, K. (1996) Glycosylation of microtubule–associated protein tau: An abnormal posttranslational modification in Alzheimer's disease. *Nat. Med.* **2**, 871
8. Dennis, J. W., Granovsky, M., and Warren, C. E. (1999) Protein glycosylation in development and disease. *Bioessays* **21**, 412–421
9. Martin-Rendon, E., and Blake, D. J. (2003) Protein glycosylation in disease: New insights into the congenital muscular dystrophies. *Trends Pharmacol. Sci.* **24**, 178–183
10. Ohtsubo, K., and Marth, J. D. (2006) Glycosylation in cellular mechanisms of health and disease. *Cell* **126**, 855–867
11. Hirabayashi, J., Hashidate, T., Arata, Y., Nishi, N., Nakamura, T., Hirashima, M., Urashima, T., Oka, T., Futai, M., Muller, W. E. G., Yagi, F., and Kasai, K.-i. (2002) Oligosaccharide specificity of galectins: A search by frontal affinity chromatography. *Biochim. Biophys. Acta* **1572**, 232–254
12. Leffler, H., Carlsson, S., Hedlund, M., Qian, Y., and Poirier, F. (2002) Introduction to galectins. *Glycoconj. J.* **19**, 433–440
13. Nabi, I. R., Shankar, J., and Dennis, J. W. (2015) The galectin lattice at a glance. *J. Cell Sci.* **128**, 2213–2219
14. Johannes, L., Jacob, R., and Leffler, H. (2018) Galectins at a glance. *J. Cell Sci.* **131**, jcs208884
15. Bresalier, R. S., Mazurek, N., Sternberg, L. R., Byrd, J. C., Yunker, C. K., Nangia-Makker, P., and Raz, A. (1998) Metastasis of human colon cancer is altered by modifying expression of the β-galactoside-binding protein galectin 3. *Gastroenterology* **115**, 287–296
16. Furtak, V., Hatcher, F., and Ochieng, J. (2001) Galectin-3 mediates the endocytosis of β-1 integrins by breast carcinoma cells. *Biochem. Biophys. Res. Commun.* **289**, 845–850
17. Ochieng, J., Furtak, V., and Lukyanov, P. (2002) Extracellular functions of galectin-3. *Glycoconj. J.* **19**, 527–535
18. Sano, H., Hsu, D. K., Apgar, J. R., Yu, L., Sharma, B. B., Kuwabara, I., Izui, S., and Liu, F.-T. (2003) Critical role of galectin-3 in phagocytosis by macrophages. *J. Clin. Invest.* **112**, 389–397
19. Partridge, E. A., Le Roy, C., Di Guglielmo, G. M., Pawling, J., Cheung, P., Granovsky, M., Nabi, I. R., Wrana, J. L., and Dennis, J. W. (2004) Regulation of cytokine receptors by golgi N-glycan processing and endocytosis. *Science* **306**, 120–124
20. Lajoie, P., Partridge, E. A., Guay, G., Goetz, J. G., Pawling, J., Lagana, A., Joshi, B., Dennis, J. W., and Nabi, I. R. (2007) Plasma membrane domain organization regulates EGFR signaling in tumor cells. *J. Cell Biol.* **179**, 341–356
21. Lakshminarayan, R., Wunder, C., Becken, U., Howes, M. T., Benzing, C., Arumugam, S., Sales, S., Ariotti, N., Chambon, V., and Lamaze, C. (2014) Galectin-3 drives glycosphingolipid-dependent biogenesis of clathrin-independent carriers. *Nat. Cell Biol.* **16**, 595
22. Mathew, M. P., Tan, E., Saeui, C. T., Bovonratwet, P., Sklar, S., Bhattacharya, R., and Yarema, K. J. (2016) Metabolic flux-driven sialylation alters internalization, recycling, and drug sensitivity of the epidermal growth factor receptor (EGFR) in SW1990 pancreatic cancer cells. *Oncotarget* **7**, 66491–66511
23. Mathew, M. P., and Donaldson, J. G. (2018) Distinct cargo-specific response landscapes underpin the complex and nuanced role of galectin-glycan interactions in clathrin-independent endocytosis. *J. Biol. Chem.* **293**, 7222–7237
24. Mathew, M. P., and Donaldson, J. G. (2019) Glycosylation and glycan interactions can serve as extracellular machinery facilitating clathrin-independent endocytosis. *Traffic* **20**, 295–300
25. Mathew, M. P., Tan, E., Saeui, C. T., Bovonratwet, P., Liu, L., Bhattacharya, R., and Yarema, K. J. (2015) Metabolic glycoengineering sensitizes drug-resistant pancreatic cancer cells to tyrosine kinase inhibitors erlotinib and gefitinib. *Bioorg. Med. Chem. Lett.* **25**, 1223–1227
26. Hughes, R. C. (1999) Secretion of the galectin family of mammalian carbohydrate-binding proteins. *Biochim. Biophys. Acta* **1473**, 172–185
27. Mehul, B., and Hughes, R. C. (1997) Plasma membrane targetting, vesicular budding and release of galectin 3 from the cytoplasm of mammalian cells during secretion. *J. Cell Sci.* **110**, 1169–1178
28. Menon, R. P., and Hughes, R. C. (1999) Determinants in the N-terminal domains of galectin-3 for secretion by a novel pathway circumventing the endoplasmic reticulum–Golgi complex. *Eur. J. Biochem.* **264**, 569–576
29. Takenaka, Y., Fukumori, T., and Raz, A. (2002) Galectin-3 and metastasis. *Glycoconj. J.* **19**, 543–549
30. Iacobini, C., Blasetti Fantauzzi, C., Bedini, R., Pecci, R., Bartolazzi, A., Amadio, B., Pesce, C., Pugliese, G., and Menini, S. (2018) Galectin-3 is essential for proper bone cell differentiation and activity, bone remodeling and biomechanical competence in mice. *Metabolism* **83**, 149–158
31. Popa, S. J., Stewart, S. E., and Moreau, K. (2018) Unconventional secretion of annexins and galectins. *Semin. Cell Dev. Biol.* **83**, 42–50
32. Bänfer, S., Schneider, D., Dewes, J., Strauss, M. T., Freibert, S.-A., Heimerl, T., Maier, U. G., Elsässer, H.-P., Jungmann, R., and Jacob, R. (2018) Molecular mechanism to recruit galectin-3 into multivesicular bodies for polarized exosomal secretion. *Proc. Natl. Acad. Sci. U. S. A.* **115**, E4396–E4405
33. Stewart, S. E., Menzies, S. A., Popa, S. J., Savinykh, N., Petrunkina Harrison, A., Lehner, P. J., and Moreau, K. (2017) A genome-wide CRISPR screen reconciles the role of N-linked glycosylation in galectin-3 transport to the cell surface. *J. Cell Sci.* **130**, 3234–3247
34. Hart, G. W., Slawson, C., Ramirez-Correa, G., and Lagerlof, O. (2011) Cross talk between O-GlcNAcylation and phosphorylation: Roles in signaling, transcription, and chronic disease. *Annu. Rev. Biochem.* **80**, 825–858
35. Hardivillé, S., and Hart, G. W. (2014) Nutrient regulation of signaling, transcription, and cell physiology by O-GlcNAcylation. *Cell Metab.* **20**, 208–213
36. Hart, G. W. (2014) Three decades of research on O-GlcNAcylation–a major nutrient sensor that regulates signaling, transcription and cellular metabolism. *Front. Endocrinol.* **5**, 183
37. Bond, M. R., and Hanover, J. A. (2015) A little sugar goes a long way: The cell biology of O-GlcNAc. *J. Cell Biol.* **208**, 869–880
38. Tazhitdinova, R., and Timoshenko, A. V. (2020) The emerging role of galectins and O-GlcNAc homeostasis in processes of cellular differentiation. *Cells* **9**, 1792
39. Keembiyehetty, C., Love, D. C., Harwood, K. R., Gavrilova, O., Comly, M. E., and Hanover, J. A. (2015) Conditional knock-out reveals a requirement for O-linked N-Acetylglucosaminase (O-GlcNAcase) in metabolic homeostasis. *J. Biol. Chem.* **290**, 7097–7113
40. Munkley, J., and Elliott, D. J. (2016) Hallmarks of glycosylation in cancer. *Oncotarget* **7**, 35478–35489
41. Peixoto, A., Relvas-Santos, M., Azevedo, R., Santos, L. L., and Ferreira, J. A. (2019) Protein glycosylation and tumor microenvironment alterations driving cancer hallmarks. *Front. Oncol.* **9**, 380
42. Hanover, J. A., Chen, W., and Bond, M. R. (2018) O-GlcNAc in cancer: An oncometabolism-fueled vicious cycle. *J. Bioenerg. Biomembr.* **50**, 155–173
43. Pravata, V. M., Omelková, M., Stavridis, M. P., Desbiens, C. M., Stephen, H. M., Lefeber, D. J., Gecz, J., Gundogdu, M., Õunap, K., Joss, S., Schwartz, C. E., Wells, L., and van Aalten, D. M. F. (2020) An intellectual disability syndrome with single-nucleotide variants in O-GlcNAc transferase. *Eur. J. Hum. Genet.* **28**, 706–714
44. Park, S. K., Zhou, X., Pendleton, K. E., Hunter, O. V., Kohler, J. J., O'Donnell, K. A., and Conrad, N. K. (2017) A conserved splicing silencer dynamically regulates O-GlcNAc transferase intron retention and O-GlcNAc homeostasis. *Cell Rep.* **20**, 1088–1099
45. Iurisci, I., Tinari, N., Natoli, C., Angelucci, D., Cianchetti, E., and Iacobelli, S. (2000) Concentrations of galectin-3 in the sera of normal controls and cancer patients. *Clin. Cancer Res.* **6**, 1389–1393

46. Sakaki, M., Oka, N., Nakanishi, R., Yamaguchi, K., Fukumori, T., and Kanayama, H.-o. (2008) Serum level of galectin-3 in human bladder cancer. *J. Med. Invest.* **55**, 127–132
47. Anand, I. S., Rector, T. S., Kuskowski, M., Adourian, A., Muntendam, P., and Cohn, J. N. (2013) Baseline and serial measurements of galectin-3 in patients with heart failure: Relationship to prognosis and effect of treatment with valsartan in the Val-HeFT. *Eur. J. Heart Fail.* **15**, 511–518
48. O'Seaghdha, C. M., Hwang, S.-J., Ho, J. E., Vasan, R. S., Levy, D., and Fox, C. S. (2013) Elevated galectin-3 precedes the development of CKD. *J. Am. Soc. Nephrol.* **24**, 1470–1477
49. Takemoto, Y., Ramirez, R. J., Yokokawa, M., Kaur, K., Ponce-Balbuena, D., Sinno, M. C., Willis, B. C., Ghanbari, H., Ennis, S. R., Guerrero-Serna, G., Henzi, B. C., Latchamsetty, R., Ramos-Mondragon, R., Musa, H., Martins, R. P., *et al.* (2016) Galectin-3 regulates atrial fibrillation remodeling and predicts catheter ablation outcomes. *JACC Basic Transl. Sci.* **1**, 143–154
50. Piper, S. E., de Courcey, J., Sherwood, R. A., Amin-Youssef, G. F., and McDonagh, T. A. (2016) Serial galectin-3 for the monitoring of optimally treated stable chronic heart failure: A pilot study. *Int. J. Cardiol.* **207**, 279–281
51. Kajitani, K., Yanagimoto, K., and Nakabeppu, Y. (2017) Serum galectin-3, but not galectin-1, levels are elevated in schizophrenia: Implications for the role of inflammation. *Psychopharmacology* **234**, 2919–2927
52. Melin, E. O., Dereke, J., Thunander, M., and Hillman, M. (2018) Depression in type 1 diabetes was associated with high levels of circulating galectin-3. *Endocr. Connect.* **7**, 819–828
53. Gupta, R. (2001) *Prediction of glycosylation sites in proteomes: From post-translational modifications to protein function*, Ph.D. Thesis at CBS
54. Gupta, R., and Brunak, S. (2002) Prediction of glycosylation across the human proteome and the correlation to protein function. *Pac. Symp. Biocomput.*, 310–322